AN EMPIRICAL MODEL TO ACCOUNT FOR DIFFERENCES BETWEEN LONGITUDINAL AND TRANSVERSE STRUCTURE FUNCTIONS DUE TO ANISOTROPY

Giovanni P. Romano, Stefano Bisceglia
Department of Mechanics and Aeronautics, University "La Sapienza"
Via Eudossiana 18, 00184 Roma, Italy
gp.romano@dma.ing.uniroma1.it

Robert A. Antonia, Tongming Zhou
Department of Mechanical Engineering, University of Newcastle
NSW 2308, Newcastle, Australia
meraa@alinga.newcastle.edu.au

ABSTRACT

In this paper the difference between scaling exponents derived from longitudinal and transverse structure functions is examined. Several flow fields are considered to relate such a difference to the Reynolds number (which reflects the small-scale anisotropy) and to the ratio between longitudinal and transverse velocity fluctuations (which depends on the large scale anisotropy). The experimental results confirm that the difference between longitudinal and transverse scaling exponents changes as a result of the previous anisotropies. It decreases with the Reynolds number and increases as the ratio of the *rms* values of the velocity fluctuations in the longitudinal and mean shear flow directions. The experimental results are in reasonable agreement with predictions from an empirical model based on the small and large scale asymptotes of structure functions.

MOTIVATION OF THE PAPER

It is well established that moments of the increment between velocity fluctuations at two points (or velocity structure functions, SF) in a high Reynolds number turbulent flow scale, albeit approximately, as a power of the separation between the points (Frisch, 1995). According to the local similarity hypothesis of Kolmogorov (K41), the scaling exponent increases linearly with the moment of the SF. In reality, the increase is non linear due to fluctuations of the energy dissipation rate, a phenomenon referred to as small scale intermittency. These departures from K41 have been extensively reported for longitudinal structure functions (LSF), that is for the statistics of the differences of velocity components along the direction of separation (Sreenivasan and Antonia, 1997).

Less attention has been given to transverse structure functions (TSF) or differences of velocity components along directions orthogonal to the separation. For locally isotropic incompressible turbulence, the second-order LSF and TSF are related by (Frisch, 1995)

$$< \delta u_T^{*2} >= \left(1 + \frac{r^*}{2} \frac{\partial}{\partial r^*} \right) < \delta u_L^{*2} >$$

where the asterisks denote normalisation by the Kolmogorov length scale ($\eta=(\nu^3/\langle\varepsilon\rangle)^{1/4}$, where $\langle\varepsilon\rangle$ is the mean turbulent energy dissipation rate) and the Kolmogorov velocity scale ($u_K=(\nu\langle\varepsilon\rangle)^{1/4}$). In the inertial range (IR) ($\eta<<r<<L$, where L is the integral length scale), structure functions are expected to scale as r^{ζ_p}. Inserting such a scaling into the previous relation, the equality between second-order exponents for LSF and TSF is derived. Although comparable results have yet to be established for $p\neq2$, extrapolation of the previous equality leads to equivalence between the absolute magnitudes of the LSF and TSF exponents. This result is not supported by the majority of the available experimental and numerical data (Boratav and Pelz, 1997; van de Water and Herweijer, 1999; Zhou and Antonia, 2000). The difference is about 20% for $p=4$ and 40% for $p=8$. This inequality clearly requires further investigation, especially in the context of improving small-scale turbulence modelling. Possible explanations, not necessarily unrelated, for this inequality are (i) the anisotropy of the flow, (ii) the Reynolds number, (iii) the initial and boundary conditions, (iv) the intermittencies affecting LSF and TSF (which may be inherently different).

Possibilities (i) and (iii) give different injections of energy at the large scales which could, in turn, affect the IR. This could explain why there is qualitative agreement for the inequality between longitudinal and transverse exponents as well as significant disagreement with regard to its magnitude. Regarding (ii), there is a tendency for the IR to contract and eventually disappear as the Reynolds number is reduced (Pearson and Antonia, 2000). Possibility (iv) has been considered, in

particular through differences in the scaling of the locally averaged energy dissipation rate and of the enstrophy, but the differences (2% for p=4 and 6% for p=8) are much smaller than measurements (Antonia, Zhou and Zhu, 1998).

The aim of the paper is to investigate the difference between LSF and TSF in the context of the anisotropy of the flow, the initial and boundary conditions and the Reynolds number. These are addressed by comparing results in several flows (jets and wakes) at different values of the Reynolds number and of the ratio u'/v' (where the prime denotes the rms value). The former is used to investigate the effect of small scales on structure functions, whereas the latter concerns with large scales. The results are compared with empirical relations derived from the small and large scale asymptotes of structure functions. The differences between LSF and TSF exponents are examined in the context of differences in either the Reynolds number or the ratio u'/v'.

EXPERIMENTAL FACILITIES

Two main experimental arrangements were used:

- air and water jets at Reynolds numbers (R_λ, based on the longitudinal Taylor microscale, λ, and on u'), between about 230 and 1000;
- different wakes (of cylinder, plate or screen) at $R_\lambda \approx 200$ with different values of u'/v'.

The air jet facility consists of an open circuit wind tunnel: after the contraction (1:85 in area) the exit diameter d is equal to 55 mm. An X-wire probe was mounted on a 2-D traversing mechanism: it has a diameter of 2.5 μm and an active length of about 0.5 mm (about 3.3 Kolmogorov microscales at the measurement station).

The water jet facility consists of a closed water circuit with a strong contraction (1:50 in area) and a diameter d =20 mm. Two-component forward-scatter mode LDA measurements were made. The fringe spacing was 3.42 μm and the measurement volume size is about 0.1mm × 0.1mm × 0.8mm. The LDA data are linearly resampled.

The wake measurements were made in a low-speed open circuit wind tunnel with a 2.4 m long test section of square cross section (350 mm × 350 mm). The floor of the test section was adjusted to achieve a zero pressure gradient. Each of the five wake generators (the vertical dimension $h \approx 25.4$ mm was the same in each case) spanned the full width of the working section. Both solid and porous bodies were used. The solid bodies included a plate mounted normal to the flow and two cylinders, with circular and square cross sections. The porous strip and circular cylinder were constructed from a screen (0.5 mm wires) of 54% solidity.

Flow	R_λ	u'/v'	L_u/L_v	η (mm)
Circular jet	230÷500	1.19	~2.34	~0.105
	280÷1000	1.33	~2.2	~0.10
Plane jet	500	1.10	1.50	0.082
	1100	1.13	1.91	0.082
Wake				
(porous strip)	≈200	0.85	7.00	0.125
(plate)	≈200	0.98	3.62	0.180
(sq. cylind.)	≈200	1.06	4.72	0.184
(porous cyl.)	≈200	1.07	9.09	0.227
(cir. cylind.)	≈200	1.11	1.13	0.195

Table 1: Experimental parameters: L_u and L_v are the integral length scales associated with u and v respectively.

In the jets, measurements were made at distances, where the flow field may be considered to be self-preserving. Because of the working section length limitation, the wake measurements were made at $x = 70h$, which is too small a distance to expect self-preservation of the Reynolds stresses. The number of samples is of the order of 5×10^5. Taylor's hypothesis is used: the LSF is obtained from temporal differences of the longitudinal component, while the TSF is inferred from the radial component. The IR (or more approximately a scaling range) is identified with the region where the third-order LSF increases linearly with r^* ($\zeta_3^L \equiv 1$). The linear relation is an exact result derived from the Navier-Stokes equations for homogeneous isotropic turbulence at high Reynolds numbers. Scaling exponents of other ($p\neq3$) structure functions, including the transverse ones, are determined by fitting data over this range.

Table 1 contains relevant experimental information. Note that the data cover at least one order of magnitude in R_λ and a significant range for the magnitude of u'/v'.

AN EMPIRICAL DESCRIPTION OF THE PTH- ORDER STRUCTURE FUNCTIONS

The major portion of the observed differences between LSF and TSF is ascribed to the large scale anisotropy. Preliminary results for the air and water jets suggest that the ratio u'/v', which is different in each flow, is an indicator of the energy supplied to the large scales. Further, Paret and Tabeling (1998) have noted that the condition of incompressibility could also cause LSF and TSF exponents to be different, owing to the different forms of the longitudinal and transverse correlation functions. These indications are grouped into an empirical model for SF scaling exponents.

Indeed, the magnitudes of second-order LSF and TSF approach $2u'^2$ and $2v'^2$ for $r^*\rightarrow\infty$. A simplistic description is given by the model proposed below.

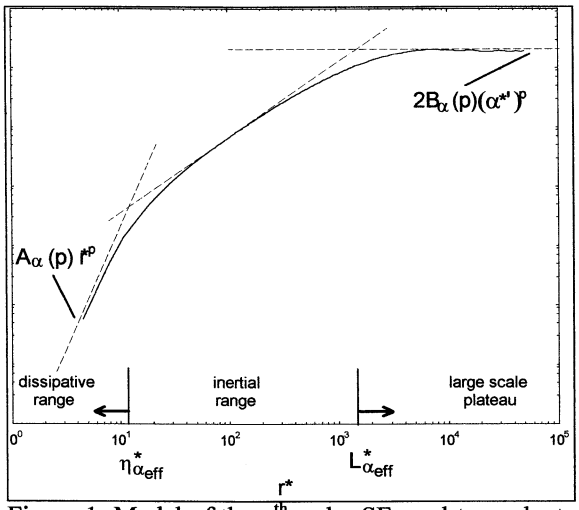

Figure 1: Model of the p[th]-order SF used to evaluate the scaling range exponents in the IR.

A necessary requirement for a model, as sketched in Figure 1, is that it should correctly reproduce the asymptotic behaviour of the p^{th}-order structure functions (Frisch, 1995)

$$< \delta\alpha^{*p} > \rightarrow A_\alpha(p) r^{*p} \qquad r^* \rightarrow 0$$
$$< \delta\alpha^{*p} > \rightarrow 2B_\alpha(p) \alpha'^{*p} \qquad r^* \rightarrow \infty$$

where $\alpha \equiv u$ or v and the pre-factors $A_\alpha(p)$ and $B_\alpha(p)$ depend on the Reynolds number. It is necessary to specify the limiting values for r^*. At the lower end, $r^* \approx 1$, whereas r^* is proportional to the integral scale L_α at the higher end. We adopt Sreenivasan's (1995) suggestion and introduce effective length scales (which are multiples of η and L_α), η^*_{eff} and $L^*_{\alpha eff}$. The scaling exponents of the p[th]-order structure function can then be approximated by

$$\zeta_p^\alpha = \frac{\log C_\alpha(p)}{\log D_\alpha}$$

where $C_\alpha(p) = (2B_\alpha(p)\, \alpha'^*) / (A_\alpha(p)\, \eta_{eff}^{*p})$ and $D_\alpha = L_{\alpha eff}/\eta_{eff}$. From the previous relation it is possible to evaluate the relative difference between longitudinal ($\alpha=u$) and transverse ($\alpha=v$) exponents. To this end, a knowledge of $A_\alpha(p)$ and $B_\alpha(p)$ is required. Assuming isotropy, for $p=2$, $A_u(2)=1/15$, $A_v(2)=2A_u(2)$, $B_\alpha(2)=1$ and $C_u(2)/C_v(2)=2(u'/v')^2$ (similar relations can be obtained for $p=4$) (Frisch, 1995). Thus the model explicitly contains the ratio u'/v', which is one measure of the large scale anisotropy. As the degree of anisotropy increases, the magnitude of the relative difference between longitudinal and transverse exponents also increases. Further, for isotropic turbulence, $C_\alpha(2) \approx R_\lambda$ and $D_\alpha \approx R_\lambda^{3/2}$ so that the dependence on the Reynolds number can be also evaluated.

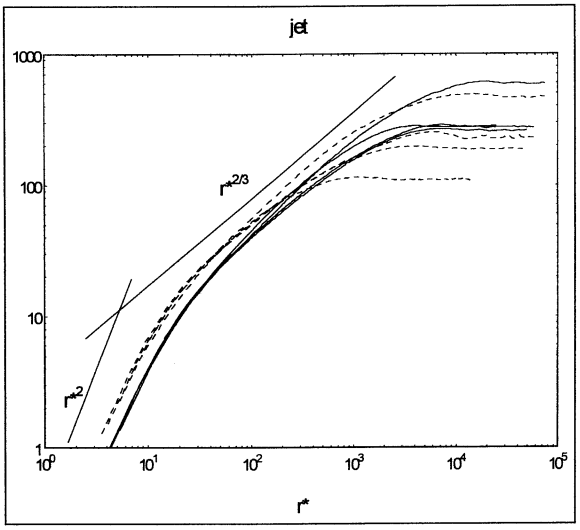

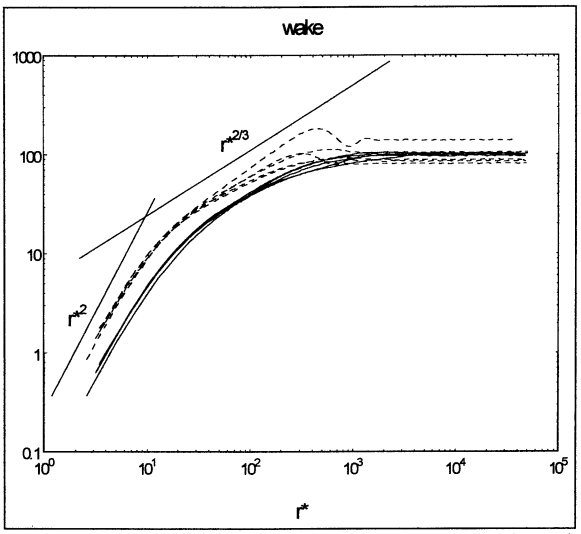

Figure 2: Second-order LSF (continuous lines) and TSF (dotted lines) for the jet flows at $R_\lambda = 500 \div 1000$ (at the top) and for the wake flows at $R_\lambda = 200$ (at the bottom).

Estimates of scaling exponents from this empirical model can be compared with experimental results obtained for different large scale anisotropies and different Reynolds numbers. The values of $\eta_{eff} \approx 10\eta$ and $L_{\alpha eff} \approx L_\alpha$ have been chosen. These choices (see Figure 1) correspond to the upper limit of the dissipative range and the beginning of the large-scale plateau.

RESULTS AND COMPARISONS

LSF and TSF are evaluated for the different flows; examples of the results obtained with the second-order are given in Figure 2. All the curves approach the power law behaviour in the dissipative range. For the jet flows, the differences in the asymptotes are observed both in LSF and TSF; they reflect the different extension of the IR which depends mainly on the Reynolds number.

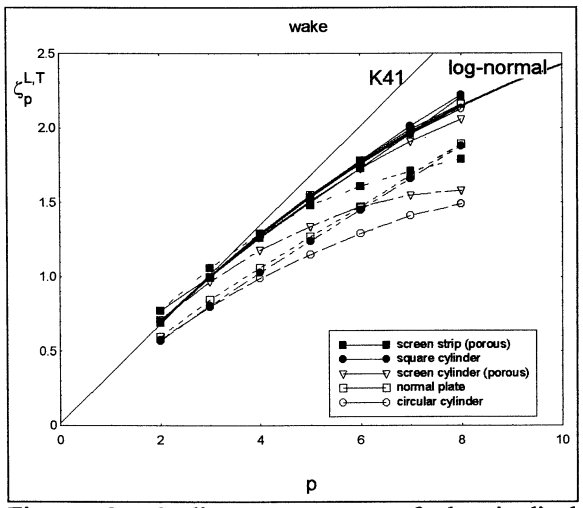

Figure 3: Scaling exponents of longitudinal (continuous lines) and transverse SF (dotted lines) for the wake flows at $R_\lambda = 200$.

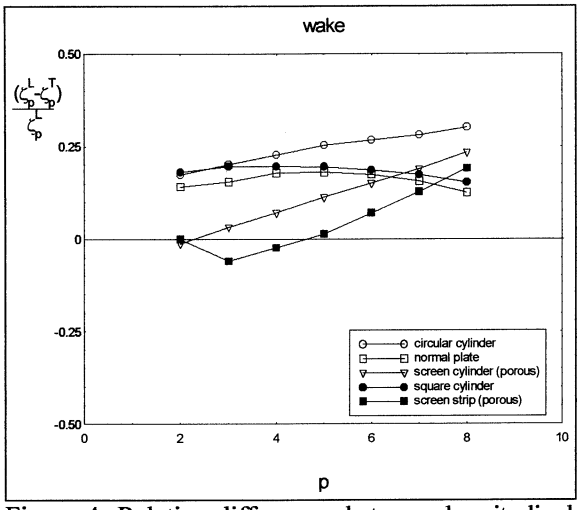

Figure 4: Relative differences between longitudinal and transverse scaling exponents for the different wake flows at $R_\lambda = 200$.

On the other hand, for the wake flows the extensions of the IR are almost the same and the LSF overlap. Changes in the TSF asymptotes are observed, reflecting the differences in large scale forcing through the variation in u'/v'. This is why the jet data will be used mainly to investigate the effect on SF of the Reynolds number while the wake data will be used to examine the influence of u'/v'.

Effect of u'/v': wake flows

From the computed LSF and TSF, the scaling exponents up to order 8 are evaluated within the IR. They are given in Figure 3 for the wake flows. While all the longitudinal exponents attain almost the same value (which is also very close to the prediction by the log-normal model also given in the figure), the transverse cover a much larger interval. The largest differences are observed for the circular cylinder for which u'/v' is largest. Therefore, the effect of the large scale forcing seems to be much more important for scaling exponents derived from TSF than for those obtained from LSF. This behaviour is observed also in the relative difference between longitudinal and transverse exponents which is shown in Figure 4. As previously noted by Romano and Antonia (2001), this difference increases with p in the jets. For the wakes, this is not always the case because, for large p, there is also a decrease for the and the square cylinder wake. In such conditions, the forcing due to transverse velocities is expected to match or even exceed that due to the longitudinal velocities. The largest relative difference is observed for the circular cylinder wake for which u'/v' is largest.

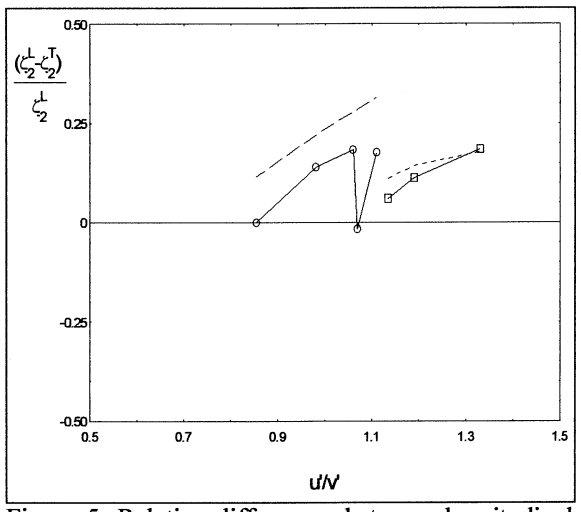

Figure 5: Relative differences between longitudinal and transverse second-order scaling exponents as a function of the ratio of velocity fluctuations for the wake flows at R_λ=200 (circles) and for the jet flows (squares). The estimates from the empirical model are also shown (dotted lines).

In agreement with this finding, the relative differences for the screen strip wake are smallest, and even change sign; in this flow, u'/v' is smallest. There seems to be a link between the magnitude of u'/v' and that of the difference between longitudinal and transverse scaling exponents. This also emerges from the previously described empirical model.

In figure 5, the relative difference between second-order scaling exponents is shown as a function of the ratio u'/v' for the different wake flows. Three points obtained from the circular and plane jet data (u'/v' = 1.13, 1.19, 1.33 see Table 1) are also included.

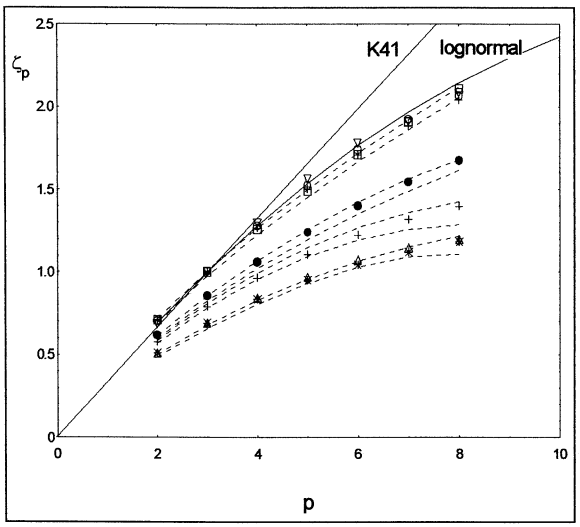

Figure 6: Scaling exponents of longitudinal and transverse SF for the jet flows at different Reynolds numbers (dotted lines are used to indicate error intervals): ∇, LSF for R_λ =280; Δ, TSF for R_λ =280; ×, LSF for R_λ =440; *, TSF for R_λ =440; □, LSF for R_λ =500; +, TSF for R_λ =500; O, LSF for R_λ =1000; ●, TSF for R_λ =1000.

The data indicate an increase in the relative difference as the large scale forcing differs for the two velocity components. When *u'/v'* is smaller than 0.9, the relative difference almost vanishes. The results from the empirical model agree well with the data; this indicates that the connection between this difference and the large scale forcing seems quite plausible.

Effect of Reynolds number: jet flows

The data from the jet flows are used to investigate the effect of the Reynolds number. In Figure 6, the LSF and TSF scaling exponents are shown for the circular water jet (the ratio between *u'* and v' is approximately constant and equal to 1.33 as given in Table 1). As for the wake flows, the LSF exponents are almost unaffected by the different values of the Reynolds number (the difference is within a few percent); they are close to the log-normal model prediction. On the other hand, the transverse exponents depart from the longitudinal as much as lower the Reynolds number. Therefore, due to the increment in the scaling range as the Reynolds number increases, the difference between longitudinal and transverse exponents decreases. This is confirmed by the analysis of the relative differences between scaling exponents which can be derived from Figure 7. As previously mentioned, such a difference increases almost linearly with p; moreover, it is almost halved at the highest Reynolds number relative to the smallest Reynolds number.

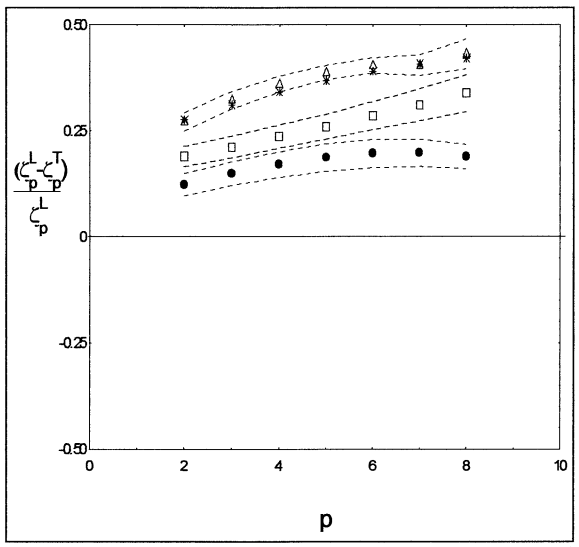

Figure 7: Relative differences between longitudinal and transverse scaling exponents for the different jet flows (dotted lines are used to indicate error intervals): Δ, R_λ =280 (1); *, R_λ =440 (1); □, R_λ =500 (1); ●, R_λ =1000 (1).

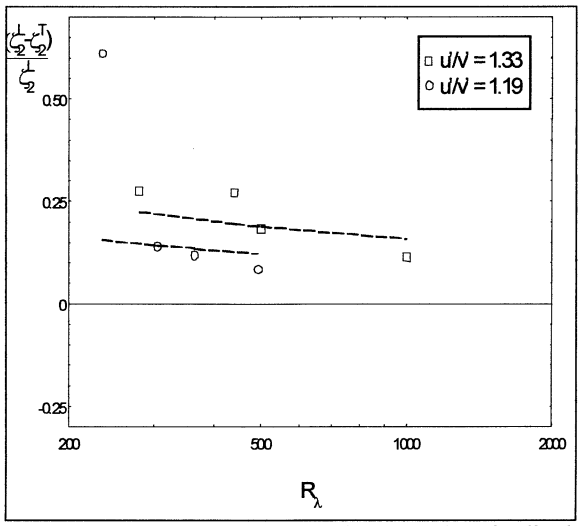

Figure 8: Relative differences between longitudinal and transverse second-order scaling exponents as a function of the Reynolds number for the jet flows. The estimates from the empirical model are also shown (dotted lines).

Thus, not only the large scales, but even the small scales play a part in determining the differences between LSF and TSF scaling exponents. In Figure 8, the relative difference between second-order scaling exponent is given as a function of the Reynolds number for the circular jet flows (at two different values of the ratio *u'/v'*). The difference clearly decreases as the Reynolds number, but does not vanish even at the highest Reynolds number. This was also observed by other authors

(Sreenivasan and Dhruva, 1998; Antonia and Pearson, 1999; Antonia, Pearson and Zhou, 2000).

As already noticed in the previous section, the difference is also a function of the large scale anisotropy through the ratio u'/v'. The trend is similar for the data acquired at the two different values of such a ratio.

CONCLUDING REMARKS

In this paper, the difference between exponents derived from the scaling of longitudinal and transverse structure functions is considered. It is well established that such exponents exhibit marked differences (larger than 30% even for low order structure functions) and that there is no agreement between results from different authors regarding the magnitude of these differences. There is however concensus on the fact that the anisotropy of the flow field must exert an influence and cannot be ignored. It is therefore, reasonable to expect this discrepancy to be also caused by differences in initial and boundary conditions; these can affect both small and large scales. Here, the focus has been on the effect of the Reynolds number on the "small" scales and the ratio u'/v' on the large scales.

Data in different wakes at about the same Reynolds number are used to examine the effect of the u'/v' ratio, whereas data from jets (circular and plane) at about the same ratio u'/v' are used to clarify the effect of the Reynolds number.

The ratio u'/v' (which contains also the effect of the large scale forcing) is shown to be a relevant parameter for the difference between longitudinal and transverse scaling exponents. When this ratio is close to 1, the difference is small, whereas when it is larger than 1 the difference increases. One may expect longitudinal exponents to become smaller than transverse exponents when $u'/v' < 1$; this needs further investigation.

As the Reynolds number increases, the region normally identified with the inertial range (in reality, an approximate scaling range) expands and the relative difference between exponents is reduced; this is in agreement with previous observations. However, the difference does not seem to vanish even when R_λ is as large as 4000.

An empirical model, based on the asymptotic behaviour of longitudinal and transverse structure functions, correctly predicts both the effect of the large scale forcing and that caused by changes in the Reynolds number.

ACKNOWLEDGEMENTS

RAA is grateful to the Australian Research Council for its support.

REFERENCES

Antonia, R.A. and Pearson, B.R., 1999, "Low-order velocity structure functions in relatively high Reynolds number turbulence", *Europhys. Lett.*, Vol. 48, pp. 163-169.

Antonia R.A., Pearson, B.R. and Zhou T., 2000, " Reynolds number dependence of second-order velocity structure functions", *Phys. Fluids*, Vol. 12, pp. 3000-3006.

Antonia, R.A., Zhou, T. and Zhu Y., 1998, "Three-component vorticity measurements in a turbulent grid flow", *J. Fluid Mech.*, Vol. 374, pp. 29-57.

Boratav, O.N. and Pelz, R. B., 1997, "Structures and structure functions in the inertial range of turbulence", *Phys. Fluids*, Vol. 9, pp. 1400-1415.

Frisch, U., 1995, "Turbulence : The Legacy of A.N. Kolmogorov", Cambridge University Press.

Paret, J. and Tabeling, P., 1998, "Intermittency in the two-dimensional inverse cascade of energy : experimental observations", *Phys. Fluids*, Vol.10, pp.3126-3136.

Pearson, B.R. and Antonia, R.A., 2000, "Reynolds number dependence of turbulent velocity and pressure increments", *J. Fluid Mech.* (submitted).

Sreenivasan K.R., 1995, "The energy dissipation in turbulent shear flows", in S. M. Deshpande, A. Prabhu, K. R. Sreenivasan and P. R. Viswanath (eds.), *Developments in Fluid Dynamics and Aerospace Engineering*, Interline Publishers, Bangalore, pp. 159-190.

Sreenivasan K.R. and Antonia, R.A., 1997, "The phenomenologyof small-scale turbulence", *Ann. Rev. Fluid Mech.*, Vol. 29, pp. 435-472.

Sreenivasan, K.R. and Dhruva, B., 1998, "Is there scaling in high-Reynolds-number turbulence?", *Prog. Theoret. Phys. Supp.*, Vol. 130, pp.103-120.

Van de Water, W. and Herweijer, J.A., 1999, "High-order structure functions of turbulence", *J. Fluid Mech.*, Vol. 387, pp. 3-37.

Zhou, T. and Antonia, R.A., 2000, "Reynolds number dependence of the small scale structures of grid turbulence", *J. Fluid Mech.*, Vol. 406, pp. 81-107.

Romano, G.P. and Antonia, R.A., 2001, "Longitudinal and transverse structure functions in a turbulent round jet: effect of initial conditions and Reynolds number", *J. Fluid Mech.*, to appear